Single-pulse stimulation of cerebellar nuclei stops epileptic thalamic activity

Rooda, O.H.J.E.; Kros, L.; Faneyte, S.J.; Holland, P.J.; Gornati, S.V.; Poelman, H.J.; ... ; Hoebeek, F.E.

Brain Stimulation 14 (2021) 861–872

Contents lists available at ScienceDirect

Brain Stimulation

journal homepage: http://www.journals.elsevier.com/brain-stimulation

Single-pulse stimulation of cerebellar nuclei stops epileptic thalamic activity

Oscar H.J. Eelkman Rooda [a, b, 1], Lieke Kros [a, 1], Sade J. Faneyte [a], Peter J. Holland [c], Simona V. Gornati [a], Huub J. Poelman [a], Nico A. Jansen [d, e], Else A. Tolner [d, e], Arn M.J.M. van den Maagdenberg [d, e], Chris I. De Zeeuw [a, f], Freek E. Hoebeek [a, g, *]

[a] Department of Neuroscience, Erasmus Medical Center, 3015, AA Rotterdam, the Netherlands
[b] Department of Neurosurgery, Erasmus Medical Center, 3015, AA Rotterdam, the Netherlands
[c] School of Psychology, University of Birmingham, Birmingham, United Kingdom
[d] Department of Neurology, Leiden University Medical Center, 2300, RC Leiden, the Netherlands
[e] Department of Human Genetics, Leiden University Medical Center, 2300, RC Leiden, the Netherlands
[f] Netherlands Institute for Neuroscience, Royal Dutch Academy for Arts and Sciences, 1105, BA Amsterdam, the Netherlands
[g] Department for Developmental Origins of Disease, University Medical Center Utrecht Brain Center and Wilhelmina Children's Hospital, Utrecht Medical Center, 3508, AB Utrecht, the Netherlands

ARTICLE INFO

Article history:
Received 20 April 2020
Received in revised form
5 April 2021
Accepted 3 May 2021
Available online 20 May 2021

Keywords:
Cerebellum
Generalized absence seizures
Optogenetic neurostimulation
Thalamus

ABSTRACT

Background: Epileptic (absence) seizures in the cerebral cortex can be stopped by pharmacological and optogenetic stimulation of the cerebellar nuclei (CN) neurons that innervate the thalamus. However, it is unclear how such stimulation can modify underlying thalamo-cortical oscillations.
Hypothesis: Here we tested whether rhythmic synchronized thalamo-cortical activity during absence seizures can be desynchronized by *single-pulse* optogenetic stimulation of CN neurons to stop seizure activity.
Methods: We performed simultaneous thalamic single-cell and electrocorticographical recordings in awake *tottering* mice, a genetic model of absence epilepsy, to investigate the rhythmicity and synchronicity. Furthermore, we tested interictally the impact of single-pulse optogenetic CN stimulation on thalamic and cortical recordings.
Results: We show that thalamic firing is highly rhythmic and synchronized with cortical spike-and-wave discharges during absence seizures and that this phase-locked activity can be desynchronized upon single-pulse optogenetic stimulation of CN neurons. Notably, this stimulation of CN neurons was more effective in stopping seizures than direct, focal stimulation of groups of afferents innervating the thalamus. During interictal periods, CN stimulation evoked reliable but heterogeneous responses in thalamic cells in that they could show an increase or decrease in firing rate at various latencies, bi-phasic responses with an initial excitatory and subsequent inhibitory response, or no response at all.
Conclusion: Our data indicate that stimulation of CN neurons and their fibers in thalamus evokes differential effects in its downstream pathways and desynchronizes phase-locked thalamic neuronal firing during seizures, revealing a neurobiological mechanism that may explain how cerebellar stimulation can stop seizures.

Introduction

Generalized epilepsy is a highly prevalent and debilitating seizure disorder involving large-scale thalamo-cortical networks [1]. Focal activity in a part of the cerebral cortex becomes hypersynchronous and rapidly spreads to large-scale networks leading to generalized seizures [2–6]. Even though many patients suffering from generalized epilepsy respond well to pharmacological

* Corresponding author. Department of Neuroscience, Erasmus Medical Center, 3015, AA Rotterdam, the Netherlands.
E-mail address: f.e.hoebeek@umcutrecht.nl (F.E. Hoebeek).
[1] These authors contributed equally.

https://doi.org/10.1016/j.brs.2021.05.002

therapy, the disorder remains refractory to drug treatment in an estimated 20–40% of patients [7,8]. For these patients neurostimulation may be an effective alternative [9,10].

Thalamic neurostimulation has been shown effective in reducing seizure occurrence in some patients with refractory epilepsy [11,12]. Stimulation of brain regions that directly project to the dorsal thalamus has been shown to ameliorate epileptic seizures in experimental settings [10,13–15]. We recently showed that optogenetic stimulation of cerebellar nuclei (CN) neurons reliably stops generalized absence seizures in mouse models [15]. At present it is unclear why this approach is so effective. Possibly, CN stimulation is efficient in stopping thalamo-cortical oscillations, because of their diverse, direct and indirect sets of innervation routes of the thalamus, exerting different effects that together can alter synchronous activity in a powerful fashion. Indeed, CN do not only directly innervate the thalamus, but they presumably also provide indirect afferent inputs via regions like the zona incerta and superior colliculus [16–18]. Here we tested whether stimulation of CN neurons, which project to the thalamus directly and indirectly via multiple routes, is more effective in stopping these presumptively synchronized oscillations than focal stimulation of different groups of isolated CN axons within the thalamus. We set out to study this in *tottering* mice, which exhibit behavioral absence seizures accompanied by electrocorticographic (ECoG) generalized spike-and-wave discharges (GSWDs) due to a P601L missense mutation in the α_{1A} subunit of voltage-gated $Ca_V2.1$ Ca^{2+} channels [19].

Our findings indicate that single-pulse optogenetic CN stimulation evokes a wide range of heterogeneous responses in thalamic relay neurons (TRN) at various latencies during interictal states and that the same stimulation can desynchronize thalamic activity during seizures, matching the highly efficient anti-seizure effect, measured in the ECoG. The high success rate of seizure disruption upon CN stimulation is not achieved by selectively stimulating subpopulations of cerebello-thalamic afferents in various thalamic nuclei.

Material and Methods

Experimental model and subject details

Data were collected from 4- to 30-week-old male and female homozygous *tottering* mice and their wild type littermates, which were kept on a C57BL/6NHsd genetic background. PCR using 5′-TTCTGGGTACCAGATACAGG-3′ (forward) and 5′-AAGTGTC-GAAGTTGGTGCGC-3′ (reverse) primers (Eurogentech, Seraing, Belgium) and restriction enzyme *Nsb*I identified the *tottering* mutation in postnatal day 9–12 tissue. All surgical and experimental procedures were performed in accordance with the European Communities Council Directive. Protocols were reviewed and approved by the institutional experimental animal committees (DEC).

Method details

Viral infection

Stereotactic viral injections were performed as previously described [15]. We bilaterally injected virus-containing solutions (100–120 nL at ~20 nL/min) to transfect neurons in the interposed and lateral CN with Channelrhodopsin-2 (AAV2-hSyn-Chr2(H134R)-EYFP) or AAV2-hSyn-EYFP in mice anesthetized with 1.5% isoflurane. After 10 min the injection pipette was slowly retracted and optic fibers (200 μm diameter; CFML22L05, Thorlabs, Newton, NJ, USA) were implanted ~200 μm above the injection site [20]. Stereotactic coordinates for CN injections were 2.5 mm posterior to lambda, 2.2 mm lateral to the midline and 2.2 mm below the pial surface. Viral vectors were originally designed by Dr. K. Deisseroth and were acquired from the University of North Carolina vector core [21]. Mice injected with viral vectors were used for both freely behaving and head-fixed experiments.

Preparation and execution of recordings in freely behaving mice

All surgical procedures were performed under isoflurane anesthesia (induction 4%; maintenance 1.5% in oxygen-enriched air). Body temperature during surgery was maintained at 37 °C by a heating pad (FHC, Bowdoin, ME, USA). Electrodes were placed at the following coordinates (mm to bregma): −1.0 AP; +3.5 ML; −0.6 DV (right S1; single 75 μm platinum (Pt)/iridium (Ir) electrodes, PT6718; Advent Research Materials, Oxford, UK); or 1.0 AP; −1.5 ML; −0.6 DV (right M1; single Pt/Ir electrodes) for LFP recordings; −1.3 AP; +1.25 ML; −3.1 DV (right VL; paired Pt/Ir); or −1.8 AP; +0.75 ML; −3.0 DV (right CL; paired Pt/Ir); or −1.8 AP; +1.6 ML; −3.0 DV (right VPL/VPM; paired Pt/Ir) for MUA recordings; two ball-tip electrodes (Ag/Ag, 75 μm) were positioned just posterior from lambda above the cerebellum to serve as reference and ground electrodes. Electrodes were connected to a 7-channel pedestal (E363/0 socket contacts and MS373 pedestal; Plastics One, Roanoke, VA, USA) and secured to the skull using light-activated bonding primer and dental cement (Kerr optibond/premise flowable, DiaDent Europe, Almere, Netherlands). Carprofen (5 mg/kg, s.c.) and Temgesic (0.1 mg/kg, s.c.) were administered for post-operative pain relief. After a recovery period (range 2.5–11 days; median 6.7 days), electrophysiological recordings were performed in freely behaving animals. Recording sessions typically took place between 9:00 and 17:00, i.e. during the light period (for further details see Ref. [22]). We visually inspected the behavior of the mice for short periods of time (i.e., usually for 15–30 min).

Preparation for head-fixed recording

ECoG electrode implantation in M1 and S1 cortices was performed as previously described [15]. To enable extracellular recordings from thalamic neurons, a subset of mice received bilateral parietal bone craniotomies (~1.5 mm diameter). In another subset of mice, the thalamic complex was implanted with optic fibers. These fibers were positioned using the following coordinates (in degrees (°) relative to the interaural axis and in mm relative to bregma): VL: 22° roll angle, −1.2 AP, −3.0 ML, −3.1 DV; VM: 2° roll angle, −1.2 AP, −1.1 ML, −3.3 DV; CL/CM: 0° roll angle, −1.3 AP, −0.75 ML, −3.0 DV; zona incerta: 0° roll angle, −2.5 AP, −1.75 ML, −3.6 DV). The exposed tissue was surrounded by a recording chamber, covered with tetracycline-containing ointment (Terra-cortril; Pfizer, New York, NY, USA) and silicon wax (Twinsil speed; Picodent, Wipperfürth, Germany). Mice were allowed to recover for more than 5 days before experiments were performed.

In vivo extracellular electrophysiology

Following a 2-hr daily accommodation session in the setup on the first two days we performed recordings in awake, head-fixed mice on the third day lasting no longer than 4 hrs. Although being head-fixed, the mice were able to move all limbs freely. We visually inspected the mice for repetitive movements during synchronous cortical activity (GSWDs), but we found no correlation [15]. For extracellular single-unit recordings, custom-made, borosilicate glass capillaries (OD 1.5 mm, ID 0.86 mm; resistance 8–12 MΩ; taper length ~5 μm; tip diameter 0.5 μm) (Harvard Apparatus, Holliston, MA, USA) filled with 2 M NaCl were

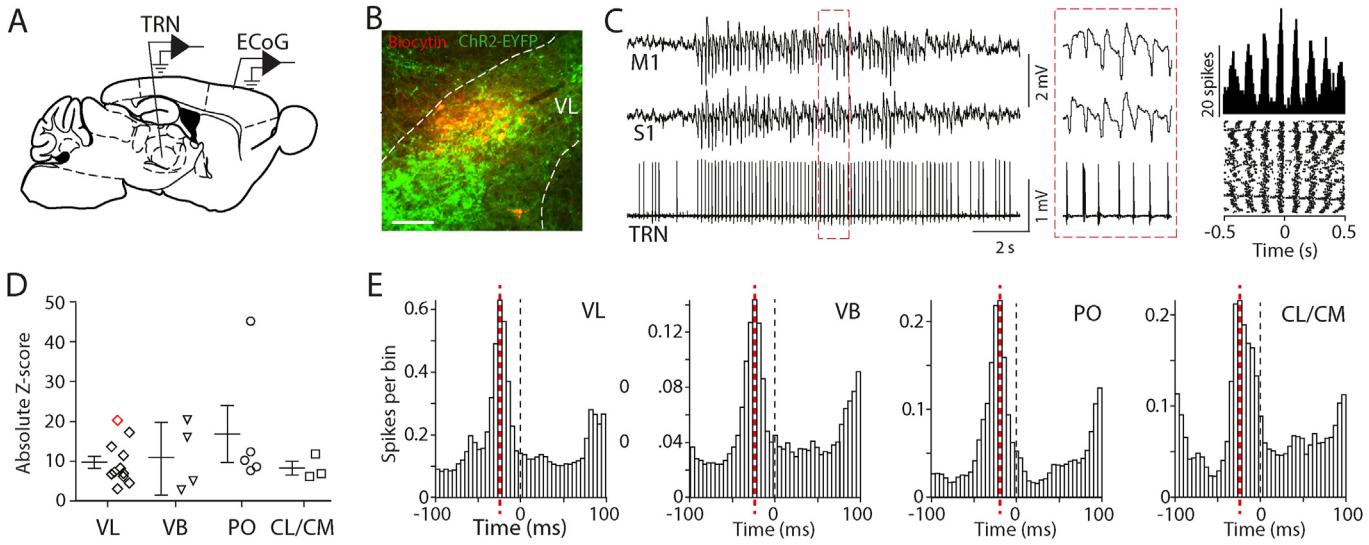

Fig. 1. Thalamic relay neurons in various nuclei show consistent phase difference with the peak of cortical GSWDs. (A) Schematic outline of head-fixed experiment for single-unit extracellular recordings from thalamic relay neurons (TRN) and multi-site ECoG recordings from M1 and S1 regions. (B) Representative image of immunohistological staining indicating the thalamic recording location (biocytin, red) in the VL nucleus that is innervated by ChR2-EYFP expressing CN axons (green). Note that in this particular image there was no signal from parvalbumin-staining visible. Scale bar indicates 50 μm. (C) (*Left*) Typical example of a TRN showing ictal activity phase-locked to GSWDs recorded from M1 and S1. In the red-dashed inset a short part of the GSWD episode is shown at a larger time scale. (*Right*) Accompanying peri-ECoG-spike-histogram and scatterplot. (D) Absolute Z-score range for GSWD-modulated TRN recordings from 8 mice (Z-score = 9.97 ± 0.99; range 1.99–47.17) for VL (n = 12 neurons), VB (n = 4 neurons), PO (n = 5 neurons) and CL/CM nuclei (n = 3 neurons). The red marker indicates the neuron shown in (C). (E) Peri-ECoG-spike histogram for all GSWD-modulated neurons recorded in VL (n = 15 cells; 7138 ECoG spikes from 3284 GSWD episodes), VB (n = 4 cells, 2064 ECoG spikes from 1369 GSWD episodes), PO (n = 5 cells, 2342 ECoG spikes from 1149 GSWDs) and CL/CM (n = 7 cells, 1645 ECoG spikes from 1066 GSWD episodes). Note the limited variability in time lag between histogram peaks (VL: 23.1 ms; VB: 16.0 ms; PO: 16.2 ms; CL/CM: 20.4 ms; as indicated by the red vertical dashed line). VL: ventrolateral; VB: ventrobasal; PO: posterior thalamus; CL: centrolateral; CM: centromedian. (For interpretation of the references to color in this figure legend, the reader is referred to the Web version of this article.)

positioned stereotactically using an electronically driven pipette holder (SM7; Luigs & Neumann, Ratingen, Germany). Stereotactic coordinates for thalamic recordings were tailored to the different thalamic nuclei and a subset of recording sites was identified using iontophoretic injections of biocytin (1.5%, ~1-min, 4-s on/off, 50% duty cycle, 4 μA), which was present in the NaCl-filled recording pipette. Thalamic neurons were considered as located in the same nucleus when recorded ≤100 μm from a marked recording site. See **Suppl. Material and Methods** for additional (interictal optogenetic) ECoG recording settings.

Optogenetic stimulation

For extracellular recordings combined with optogenetic CN or thalamic stimulation brief pulses (50 ms) of blue (470 nm) light were used to activate ChR2-infected CN neurons. Optic fibers (for CN stimulation: inner diameter 200 μm, numerical aperture (NA) 0.39; for thalamic stimulation: inner diameter 105 μm, NA 0.22; Thor Labs Newton, NJ, USA) were placed ~200 μm from the injection site and connected to 470 nm LED sources (Thor Labs). Light intensity at the tip of the implantable fiber was 550 ± 50 μW/mm^2. We chose these optic fiber diameters guided by the estimated light intensity in the brain [23] so as to ensure that in CN sufficient neurons would be activated and that in thalamus a sufficient number of CN axons were activated. LEDs were activated for 50 ms at 0.2 Hz or by a closed-loop GSWD-detection system [15,24]. In both head-fixed and freely behaving experiments we ensured that the optical stimulation did not induce gross motor movements.

Pharmacological modulation of CN neurons

The procedure to increase CN action potential firing was performed as described previously [15,24]. Briefly, we located CN neurons after which we recorded 1 hr of 'baseline' ECoG. After this, an injection was made with 100 μM gabazine ($GABA_A$-antagonist SR-95531; Tocris) dissolved in saline combined with a fluorescent dye (Evans Blue; 1% in saline) for histological verification. Next, we recorded thalamic activity for 30 min, starting 20 min after the gabazine injection, to assure the diffusion of gabazine throughout the CN. The data on GSWD-occurrence following gabazine injection from 4 out of the 6 mice have been reported previously (cf. Fig. 2 in Ref. [15]).

Immunohistochemistry

Animals were anesthetized with pentobarbital (0.15 mL, intraperitoneal) and perfused transcardially with saline followed by 4% paraformaldehyde (Sigma-Aldrich) in 0.1 M phosphate buffer (Sigma-Aldrich, pH 7.4) as previously described [15]. See for further information **Suppl. Material and Methods**.

Quantification and statistical analysis

Offline GSWD and extracellular action potential analysis

Extracellular recordings and spontaneous GSWD characteristics were analyzed offline using previously described methods [15]. In brief, action potential analysis was performed using the custom-written Matlab-based program SpikeTrain (Neurasmus, Erasmus MC Holding, Rotterdam, the Netherlands). Extracellular recordings were included if activity was stable for at least 100 s. GSWD analysis was performed using a custom-written GSWD detection algorithm (LabVIEW, National Instruments, Austin, TX, USA). Coefficient of variance (CV) was calculated as the ratio between the mean and the standard deviation of the interspike intervals (σ_{ISI}/μ_{ISI}), CV2 as (2|ISI_{n+1}-ISI_n|/(ISI_{n+1}+ISI_n)) [25] and burst index as BI = number of action potentials within bursts/total number of action potentials)

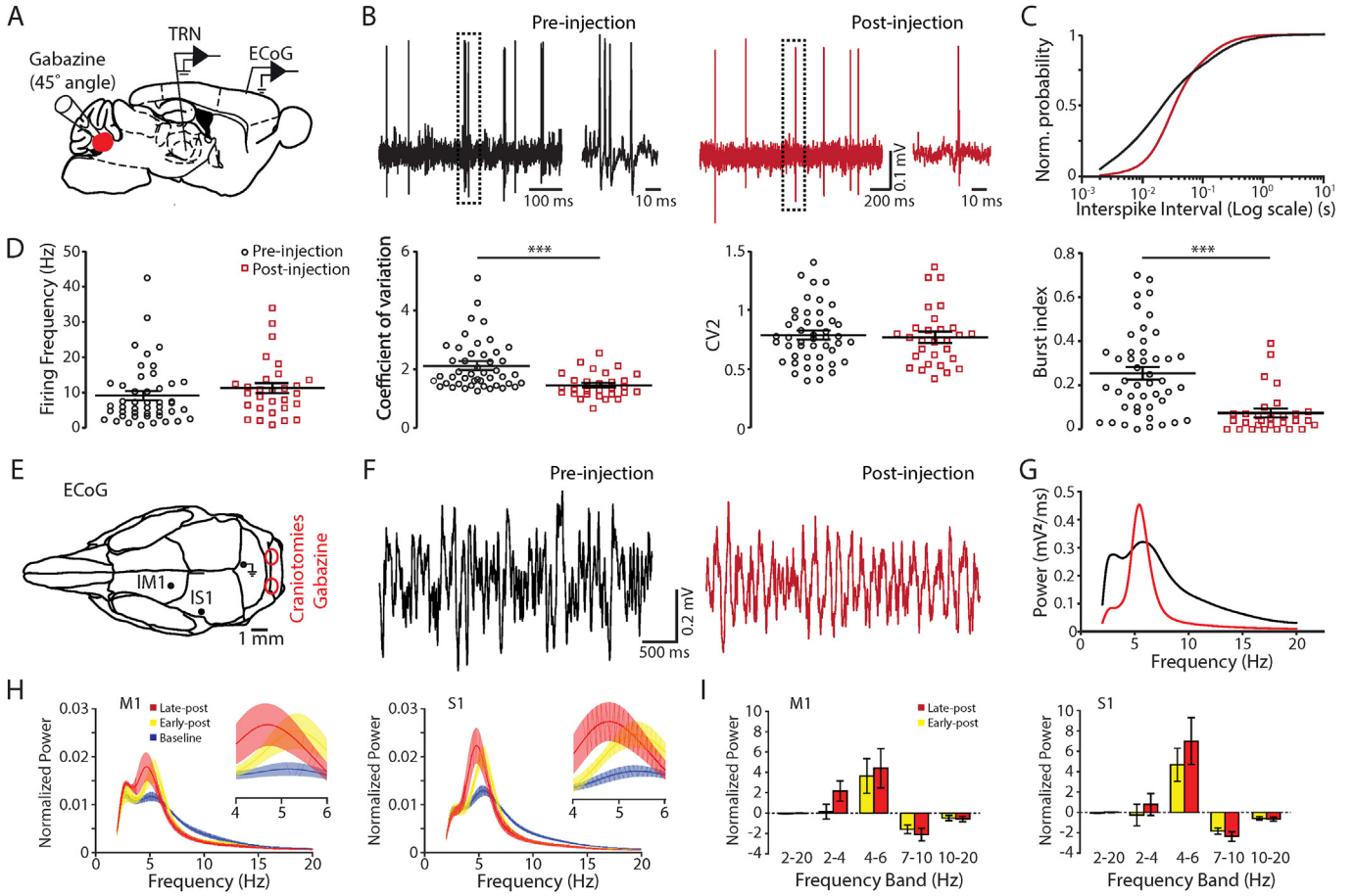

Fig. 2. Long-term modulation of cerebellar output by bilateral gabazine injections. (A) Schematic representation of the experimental design showing bilateral gabazine injections in the CN, single-unit extracellular recordings from thalamic relay neurons (TRN) and multi-site ECoG recordings from M1 and S1. (B) Example traces of two single-unit TRNs: one prior to (pre-injection; black) and just after (post-injection; red) bilateral gabazine injection in the CN. Note the presence (left trace) and absence (right) of burst-firing. (C) Accompanying normalized cumulative distribution for the interspike interval of thalamic neurons pre-injection (black) and post-injection. (D) Average firing frequency, CV, CV2 and BI calculated for neurons recorded pre- (n = 46 neurons, N = 4 mice) and post-injection (n = 29 neurons, N = 4 mice). (E) Locations of craniotomies for ECoG recording electrodes and gabazine injections into the CN. (F) Four seconds of M1 ECoG recording pre-gabazine (*left*, black) and post-gabazine (*right*, red) from a single mouse. (G) Result of fast-Fourier transform of pre-gabazine (black) and post-gabazine (red) M1 ECoG. (H) Normalized ECoG power in M1 (*left*) and S1 (*right*) recordings from 4 mice, comparing pre-gabazine (baseline), ~5–20 min after gabazine (early-post) and ~1 hr after gabazine (late-post). The insets show the normalized ECoG power in the θ-band. (I) Relative change in ECoG power (normalized to pre-gabazine condition) showing an increase in θ- (4–6 Hz) power and a significant decrease in the β-band (10–20 Hz) and the θ*-band (7–10 Hz). The power in δ- (2–4 Hz), γ (25–40 Hz) and broadband 2–20 Hz activity was not affected. Note that there was no difference between M1 and S1 responses (see also [48]) and thus for statistical comparison we grouped the M1 and S1 data. The statistical differences reported in Suppl. Table 3. *** indicate $p < 0.001$. See also Suppl. Table 2 for statistics. (For interpretation of the references to color in this figure legend, the reader is referred to the Web version of this article.)

for which we defined 'burst' as a sequence of ≥3 spikes within 100 ms.

Offline multi-unit activity analysis

Multi-unit activity (MUA) data were analyzed using the template-matching method for spike sorting with an optimal spike threshold of 3X SD from a 60-s baseline recording. Sorted spikes were exported and analyzed following a custom-written algorithm in MATLAB to generate spike histograms. The spike-to-spike correlation (autocorrelation) was calculated based on a previous method [26]. Data points (x) were normalized (X_s) in a (0,1) range using the maximum and minimum spike count (x_{max}, x_{min}): $X_s = x\text{-}x_{min}/x_{max}\text{-}x_{min}$. Mean correlation values were calculated by taking the ratio of the maximum correlation and the value at t = 0. The same time range was used to determine the maximum correlation in baseline and post-stimulation. Trials including seizures that ended −10 ms before stimulation and 150 ms after stimulation were not analyzed.

Assessment of modulation of TRN units

GSWD triggered raster plots and peri-stimulus-time-histograms (PSTHs; 5-ms bin-width) were used to calculate the modulation amplitude and frequency. ISIs of the data used for the raster plots were subsequently shuffled randomly 500X to create a normal distribution of modulation amplitudes. Cells were considered GSWD-modulated if the modulation amplitude was significantly higher than expected by chance, as indicated by a Z-score ($Z=(X-\mu)/\sigma$; $Z \geq 1.96$, $p \leq 0.05$) using the shuffled data as described previously [15], and if cells modulated at seizure frequency (6–9 Hz). The phase difference between the occurrence of the most negative deflection of a GSWD-episode and the time of the peak in thalamic activity was calculated by dividing this time difference by the median time difference between GSWDs in that particular seizure. Note that our analysis script identifies the GSWDs, then isolates ECoG spikes and finally quantifies the relative timing between the ECoG spike and thalamic action potentials. In case there are no action potentials fired, the ECoG spike is discarded for further analysis.

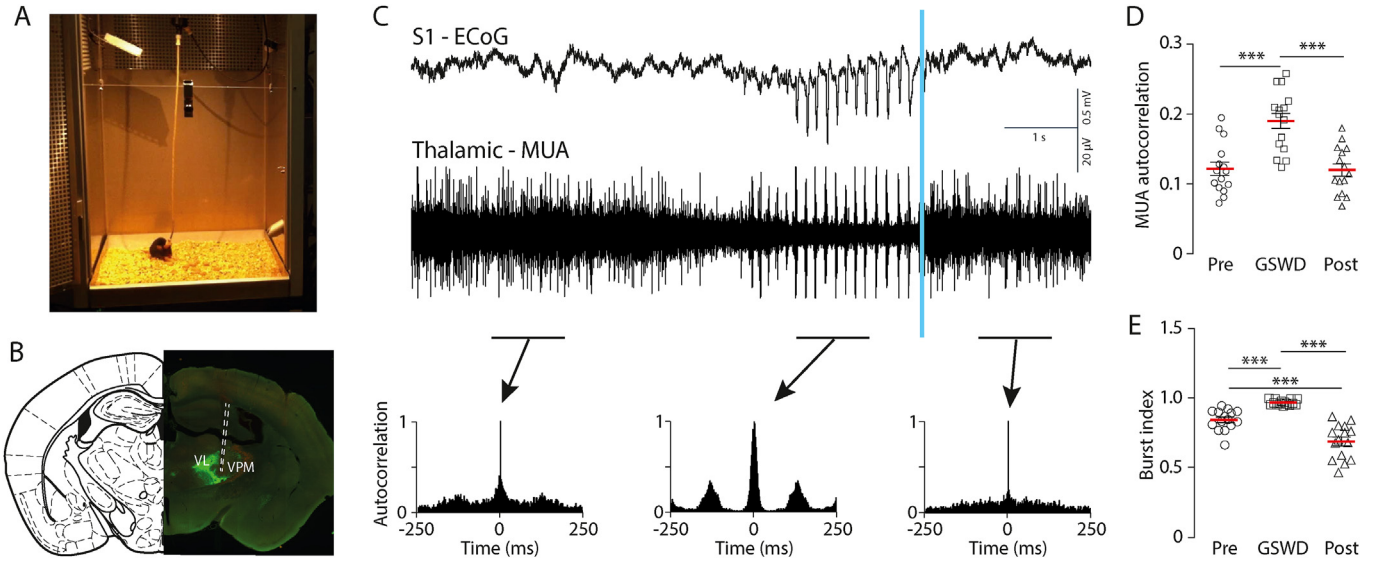

Fig. 3. Single-pulse optogenetic CN stimulation stops seizure-related rhythmic thalamic spiking. (A) Tethered recording system for simultaneous optogenetic CN stimulation, thalamic neuronal multi-unit activity (MUA) and ECoG recordings from primary motor (M1) and sensory (S1) cortices in freely behaving *tottering* mice. See Suppl. Fig. 3 for histological verification of MUA electrode placement. (B) ChR2-EYFP-expressing CN axons in the thalamic complex. The location of the bipolar MUA electrode is indicated by white-dashed lines. (C) (*Top - middle*) Example of generalized spike-and-wave discharges (GSWDs) in S1-ECoG (*top*) in synchrony with thalamic MUA (*middle*), coinciding with behavioral arrest. Single-pulse optogenetic CN stimulation (vertical blue line; 50 ms, 470 nm, 0.5 mW/mm^2) activated by a closed-loop GSWD-detection system [15,24] stopped burst firing in thalamic neurons and ended the GSWDs, upon which behavioral arrest typically ended. On average, GSWDs occurred every 72.6 ± 19.8 s (N = 8 mice, 1-hr recording per mouse). (*Bottom*) Accompanying normalized autocorrelograms of MUA in 1-s periods of pre-GSWD, GSWD and post-GSWD phases. (D) Average MUA autocorrelation for pre-GSWD, GSWD and post-GSWD multi-unit recordings. (E) As in (D) but for burst index. Data are represented as mean ± SEM. * indicates $p < 0.05$, *** indicate $p < 0.001$ (see Suppl. Table 4 for statistics). (For interpretation of the references to color in this figure legend, the reader is referred to the Web version of this article.)

Electrophysiological response to optogenetic stimulation

To determine if thalamic single units showed a significant response to optogenetic CN stimulation, we performed a random permutation calculation following a Monte-Carlo Bootstrap method, using 2-ms bin-width PSTHs. For every recording we calculated the ISIs of action potentials 4 s prior to every pulse and combined them in a single ISI distribution, which was randomly permutated 250 times. We created PSTHs from these 'fake' spike times and calculated the average and standard deviation. If the PSTH of the 'true' spiking response to optogenetic stimuli exceeded the mean ± 2 SD threshold we noted the recording to have an increased firing response. For a subset of neurons we noticed a compelling inhibition. We marked the recording as showing an inhibitory response if at any time during the post-stimulus period (5 s in total) the spike count was zero for at least 25 consecutive bins, i.e. 50 ms.

Statistical analysis

We examined the degree of normality of distributions and equality of variances in each group using Kolmogorov-Smirnov and Shapiro-Wilk's tests. We analyzed the data using parametric (paired *t*-tests, (repeated measures) ANOVAs or MANOVAs) or non-parametric tests (Kruskal Wallis tests, Mann-Whitney U tests or Friedman ANOVA's) depending on whether data were normally distributed and variances equal. Tamhane and Bonferroni corrections were used in case of multiple non-independent variables. For the ECoG data, statistical analysis of the power in each frequency band was carried out using repeated measures ANOVAs with time point ('Baseline', 'Early-Post' and 'Late-Post') as the within-subject factor and recording location as the between subject factor. Only frequency bands that displayed a significant main effect of time point were subjected to post-hoc paired *t*-tests. Two tailed testing was used in all analyses and a *p*-value ≤ 0.05 (α) was considered significant. A single asterisk indicates $p < 0.05$, two asterisks indicate $p < 0.01$, and three asterisks indicate $p < 0.001$. Details of each statistical test performed are given in **Supplementary Tables.**

Data availability

Further information and requests for data, resources and reagents should be directed to the corresponding author, Freek E. Hoebeek (f.e.hoebeek@umcutrecht.nl).

Results

Subportion of thalamic firing is rhythmic and synchronized with cortical GSWDs

Recently, we showed that optogenetic stimulation of CN neurons effectively stops generalized seizures in mouse models, implying that the CN may be a novel therapeutic target for brain stimulation for refractory epilepsy in patients [15]. To enable an in-depth investigation of mechanisms underlying this therapeutic effect, we simultaneously recorded individual thalamic neurons and cortical ECoG in awake head-fixed homozygous tottering mice. We first studied their regular seizure-related activity in the thalamic nuclei that are known to receive CN projections. Cortical GSWDs, characteristic of absence epilepsy, were detected in the ECoG signals when a seizure occurred. In this setup, seizures lasted 3.05 ± 1.00 s and consisted of repetitive ECoG spikes at 8.40 ± 0.71 Hz (N = 8 mice), which is comparable to previous studies in *tottering* mice [15,19,27,28]. Recording sites of thalamic neurons (n = 70 neurons; N = 8 mice) were labeled using iontophoretic injections of biocytin (Fig. 1A and B). From an additional 52 thalamic neurons (identified by their firing characteristics) we did not label the recording site. Out of the in total 122 thalamic neurons, 68 (55,7%) showed firing that was phase-locked to GSWDs (Fig. 1C and D; Suppl. Fig. 1; Suppl. Table 1). The compiled spiking

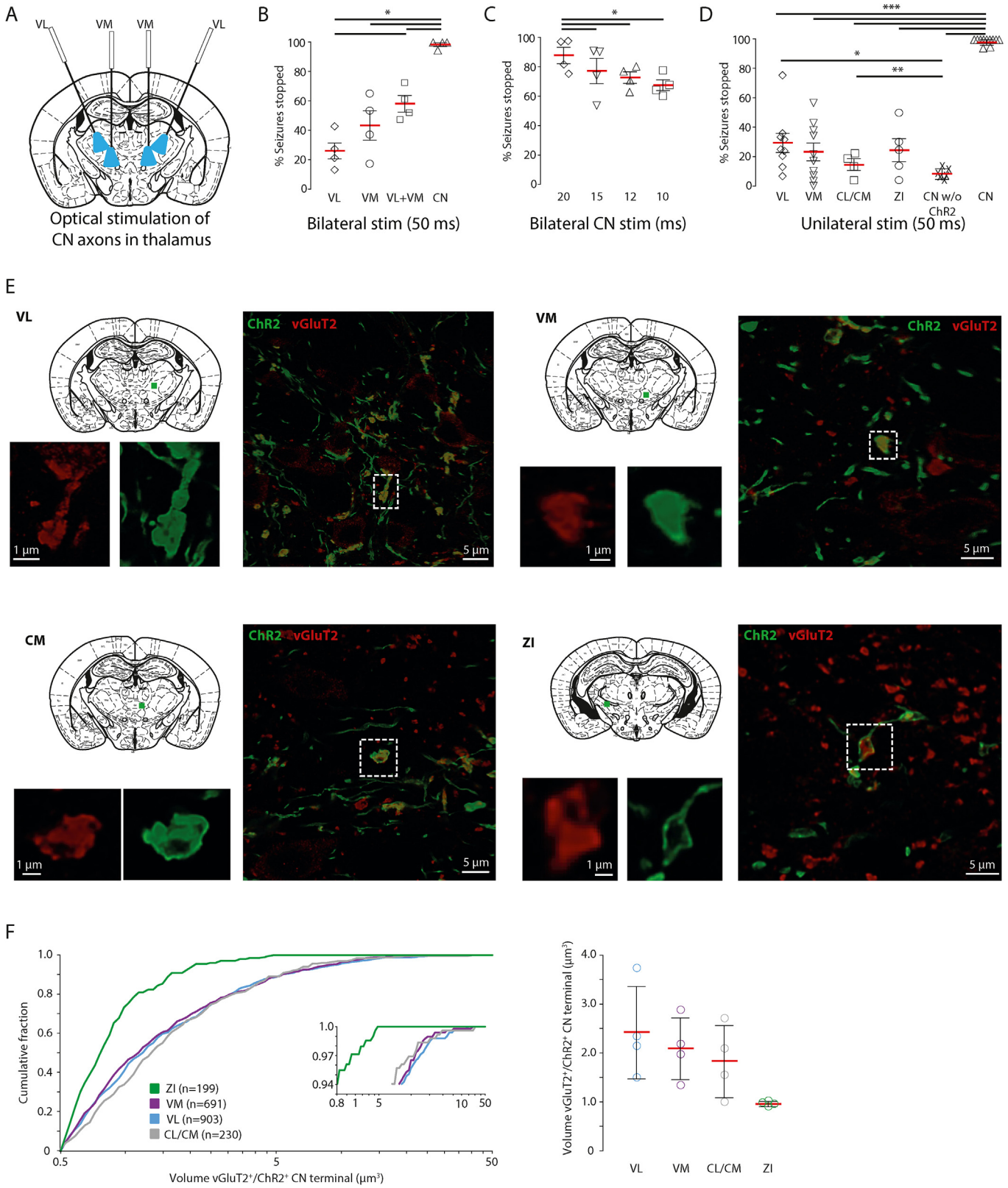

Fig. 4. Activation of cerebellar afferents in thalamic nuclei is less efficient in stopping GSWDs compared to direct CN stimulation. (A) Experimental design with four optic fibers implanted in thalamic nuclei. (B) Proportion of the seizures that stopped following bilateral VL (bilateral VL 25.8 ± 1.8% N = 4 mice; 244 seizures), bilateral VM (56.2 ± 6.0% N = 4 mice; 185 seizures), quadruple VL/VM (57.3 ± 3.9%, N = 4 mice, 250 seizures) or bilateral CN stimulation (98.7 ± 1.3% N = 4 mice; 3254 seizures) activated by a closed-loop GSWD-detection system [15,24]. (C) Proportion of seizures terminated upon bilateral CN stimulation with varying pulse lengths. Data from the same mice as reported in B. Note that at 10-ms pulse length, CN stimulation is still effective in stopping most seizures. (D) Proportion of the seizures that stopped following unilateral zona incerta (ZI) (24.4 ± 7.8%; N = 5 sites in N = 4 mice; 302 seizures), CL/CM (16.8 ± 2.2%, N = 4 sites in N = 4 mice; 205 seizures), VL (31.7 ± 2.7%, N = 9 sites in N = 5 mice, 281 seizures), VM (32.9 ± 5.0%, N = 10 sites in N = 6 mice, 417 seizures), CN stimulation (98.0 ± 1.9%, N = 11 sites in N = 6 mice, 199 seizures), or CN stimulation without ChR2-expression (8.2 ± 3.6%, N = 6 sites in N = 3 mice,

activity per nucleus shows that the phase difference between the thalamic modulation peak and ECoG spike is remarkably consistent across nuclei (Fig. 1E). Of note is that often ECoG spikes were not accompanied by thalamic action potential firing.

Pharmacologically increasing CN activity reduces thalamic burst firing and power in ECoG frequency bands

Our previous findings indicate that blocking GABAergic transmission in the CN, which increases firing frequency and regularity, decimates seizure occurrence in *tottering* and *C3H/HeOuJ* mice [15]. To further unravel the impact of modifying CN output on thalamic firing activity, we investigated the effects of gabazine infusion in the CN of *tottering* mice on interictal thalamic firing patterns and ECoG signals. Single-unit thalamic recordings indicated that bilateral infusion of gabazine in CN significantly increased the spiking regularity (CV-pre: 2.12 ± 0.12 vs. CV-post: 1.46 ± 0.08; $p < 0.001$; BI-pre: 0.25 ± 0.03 vs BI-post: 0.07 ± 0.02; $p < 0.001$), but did not alter the firing frequency (9.1 ± 1.3 Hz vs. 11.0 ± 1.5 Hz; $p = 0.328$). (Fig. 2A–D; Suppl. Table 2). In parallel, the power of ECoG frequency bands showed significant changes mediated upon pharmacological manipulation of CN firing (Fig. 2E–G). Most notably, the power of ECoG frequencies in the seizure-related high-theta band (θ*; 7–10 Hz) was significantly decreased, whereas it was increased in the low-theta band (θ; 4–6 Hz) in both M1 and S1 (Fig. 2H and I; Suppl. Table 3). Together these data indicate that long-lasting increases in CN regularity and firing frequency increases the regularity of thalamic neurons and dampens ECoG activity in seizure-related frequency bands during interictal periods.

Optogenetic CN stimulation reduces thalamic synchronization and burst firing

Next, we determined how short-lasting, single pulses of optogenetic CN stimulation affect thalamic firing during GSWDs. For this, we used MUA recordings of thalamic neurons in freely moving *tottering* mice, which showed that the rhythmicity of thalamic action potential firing was increased during GSWDs compared to interictal periods and that these oscillations were phase-locked to the ECoG spikes (Fig. 3A–C). Visual inspection of *tottering* mice showed that during GSWDs the mice were immobile. The average occurrence of GSWDs in this freely behaving setup was 18.9 ± 1.9 per hr and the average duration per episode was 2.33 ± 0.19 s. To apply optogenetic stimulation we infected CN neurons with ChR2 via AAV injections and implanted optical fibers to excite these neurons with 470 nm light pulses (0.5 mW/mm^2) of 50-ms (see Suppl. Fig. 2 for topographic mapping of ChR2-expressing CN neurons). Such optical stimulation during seizures (see Fig. 3 in Ref. [15] for controls) often triggered exploratory behavior while the phase-locked thalamic MUA was instantly reverted into a desynchronized state without rhythmic MUA bursts, as shown by a significant reduction in the peak of the MUA autocorrelogram (MUA–autocorrelation-Pre: 0.12 ± 0.01; MUA-autocorrelation-GSWD: 0.19 ± 0.01; MUA-autocorrelation-Post: 0.12 ± 0.01; Pre vs. Post $p = 0.80$; all other comparisons $p < 0.001$; Fig. 3C and D; Suppl. Fig. 3 for location of thalamic MUA electrodes; Suppl. Table 4). Likewise thalamic BI values significantly increased during GSWDs and decreased upon CN stimulation (BI-Pre: 0.85 ± 0.02; BI-GSWD: 0.97 ± 0.01; BI-Post: 0.69 ± 0.03; all comparisons $p < 0.001$; Fig. 3E; Suppl. Table 4). These findings indicate that single-pulse, yet conjunctive stimulation of the CN neurons desynchronizes seizure-related rhythmic thalamic MUA.

Stimulation of CN neurons is more effective in stopping GSWDs than activation of sets of CN axons within thalamus

CN axons synapse divergently throughout various nuclei of the thalamic complex of wild type rodents [16,18,29]. To confirm the projection patterns in *tottering* mice, we qualitatively evaluated the location of ChR2-expressing CN axons and found EYFP fluorescence in VL and VM, but also the CL, CM and ZI nuclei (Suppl. Information related to Fig. 4) alike wild type mice. To investigate whether stimulation of cerebellar afferents in thalamic nuclei is as effective in stopping GSWDs as direct stimulation of the CN, we implanted optic fibers in different nuclei of the thalamic complex of head-fixed *tottering* and optogenetically stimulated the local CN axons (see Suppl. Fig. 2 for topographic mapping of ChR2-infected CN neurons). We initially focused on VL and VM, i.e., the thalamic nuclei with the highest level of fluorescence evoked by AAV-ChR2-EYFP expressing CN axons (VL: 47.5 ± 11.2 arbitrary units (a.u.); VM: 54.5 ± 14.0 a.u.; N = 5 mice). Given that VL and VM not only innervate M1, but also prefrontal, sensory and associative cortical regions [30,31], we hypothesized that selectively stimulating CN axons in these nuclei would be sufficient to stop all GSWDs.

Using our previously published closed-loop GSWD detection system [15,32] we drove the optical stimulation and found that bilateral optogenetic stimulation of cerebellar afferents in VL or VM stopped only a portion of the seizures (VL: 26.2 ± 6.3% seizures stopped; VM: 43.4 ± 10.4%; see Suppl. Table 5 for number of seizures analyzed per animal; Fig. 4A and B). In an attempt to increase the efficacy of seizure termination we activated all thalamic optic fibers simultaneously, which was more effective (VL + VM: 58.5 ± 5.5% seizures stopped; VL vs. VL + VM $p < 0.05$), but still significantly less effective than CN stimulation (98.7 ± 1.3%; all comparisons $p < 0.05$) (Fig. 4B; Suppl. Information; Suppl. Table 6). Even when we decreased the pulse length in steps to 10 ms, the efficacy of direct CN stimulation in stopping GSWDs (71.4 ± 6.8% for 10-ms stimulation) was at least as high as when applying 50-ms pulses to the VL and VM optic fibers simultaneously (Fig. 4B and C; Suppl. Table 6). As additional controls, we also implanted fibers in the zona incerta and in the intralaminar CL and CM nuclei, all of which may also influence cortical seizure activity [33,34] and in the CN of mice injected with an AAV-EYFP construct. Optical stimulation of ChR2-expressing CN axons with 50 ms pulses of 470 nm in unilateral CL/CM and zona incerta was not as effective as unilateral stimulation of CN neurons (all comparisons $p < 0.001$) and proved only marginally better than CN stimulation in the absence of ChR2 (Fig. 4D; Suppl. Information; Suppl. Table 6). To investigate the size of the CN axon terminals in these thalamic nuclei we next used immunofluorescent staining for vesicular glutamate transporter

286 seizures. Data are represented as mean ± SEM. * indicates $p < 0.05$, *** indicate $p < 0.001$ (see Suppl. Table 5 for number of GSWDs per mouse per stimulus condition and Suppl. Table 6 for statistics). See Suppl. Information for anatomical data for location of optic fibers in thalamic nuclei. (E) stereotactic atlas [63] and confocal microscopy images of ChR2-expressing (green) CN terminal in tissue immunohistochemically stained for vesicular glutamate transporter type 2 (vGluT2; red), including a high-magnificantion of a single terminal. The microscopic images are single slices from a z-stack. (F) (*left*) Cumulative distribution of the terminal volume of all the ChR2-expressing CN terminals that colocalized with vGluT2-staining from 4 *tottering* mice (see Suppl. Material and Methods and ref [16] for technical details). (*Right*) Average terminal per thalamic terminal calculated (N = 4 mice). See Suppl. Table 7 for statistical data. VL: ventrolateral; VM: ventromedial; CL: centrolateral; CM: centromedian. (For interpretation of the references to color in this figure legend, the reader is referred to the Web version of this article.)

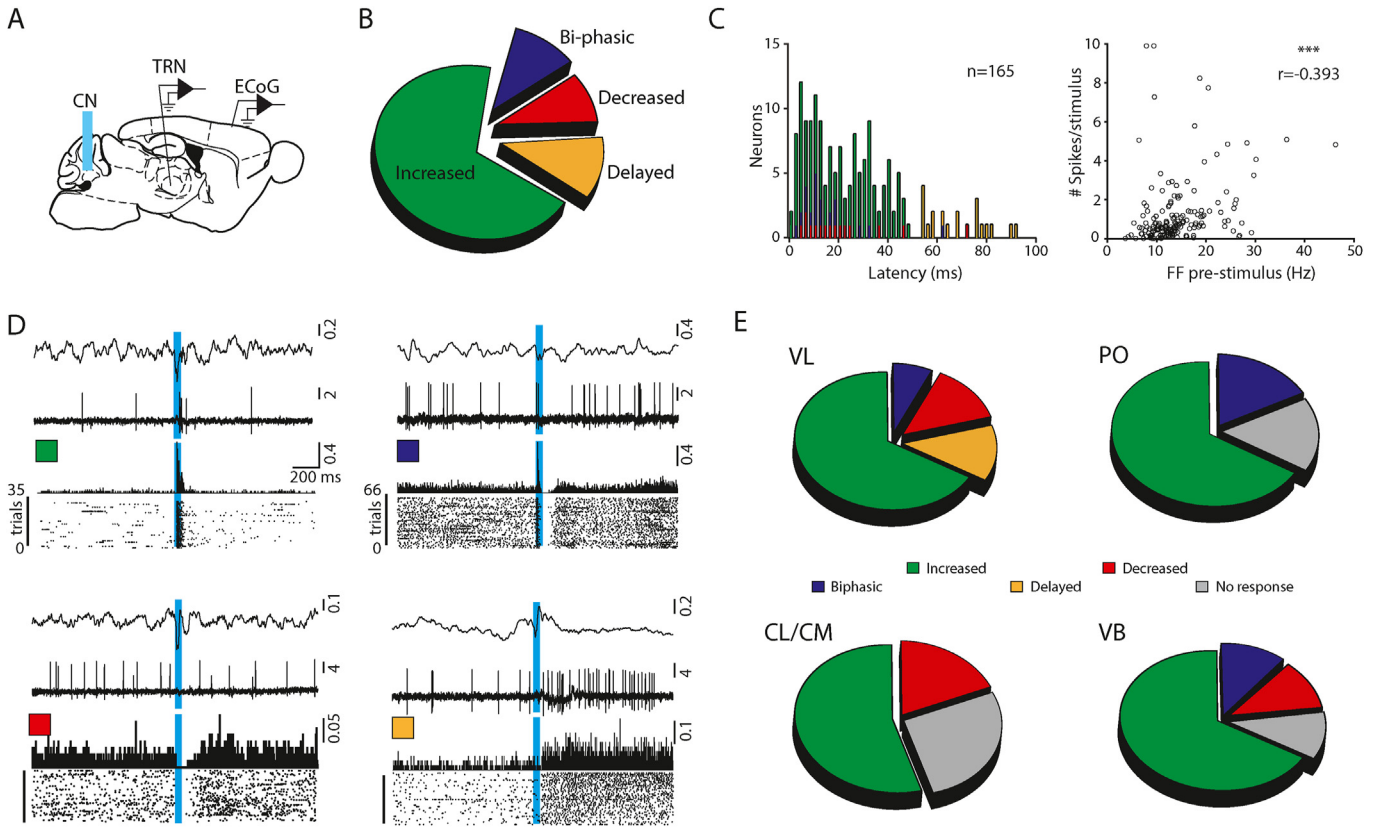

Fig. 5. CN stimulation induces variable changes in interictal thalamic firing patterns. (A) Schematic representation of simultaneous optogenetic CN stimulation (50-ms pulse of 470 nm and 0.5 mW/mm^2 at 0.2 Hz), single-unit extracellular recordings from thalamic relay neurons (TRN) and multi-site ECoG recordings from M1 and S1in head-fixed *tottering* mice. (B) Distribution of response types for 165 thalamic neurons that showed a significant response to CN stimulation (as determined by Z-score based diagnostics; see methods). See main text for the number of cells per type of response. (C) (*Left*) Histogram of response latencies of thalamic neurons (n = 165 neurons) to single-pulse (50 ms) CN stimulation (see color code of panel B). (*Right*) Scatterplot of the correlation between the pre-stimulus firing frequency (FF) and the number of spikes recorded during CN stimulation (Pearson's correlation coefficient: $r = -0.393$; $p < 0.001$). (D) For 4 different thalamic neurons a single recording trace, a per-stimulus histogram and a raster plot are shown with the accompanying ECoG (*top traces*), revealing different types of thalamic spiking patterns. Vertical scale bars are in mV. Green: 'increased' (see also Suppl. Fig. 4B); blue: 'bi-phasic' (see also Suppl. Fig. 4C); red: 'decreased' (see also Suppl. Fig. 4D); and orange: 'delayed' (see also Suppl. Fig. 4E). Vertical blue lines indicate the timing of optogenetic CN stimulation (pulse length 50 ms). (E) Proportions of neurons in VL (n = 20 neurons), VB (n = 9 neurons), PO (n = 6 neurons) and CL/CM (n = 11 neurons) that showed an 'increase', 'decrease', 'bi-phasic' or 'delayed' response upon single-pulse CN stimulation. See Suppl. Information for histological verification of recordings site and analysis of individual recordings. VL: ventrolateral; VB: ventrobasal; PO: posterior thalamus; CL: centrolateral; CM: centromedian. (For interpretation of the references to color in this figure legend, the reader is referred to the Web version of this article.)

type 2 (vGluT2). For 4 mice we labeled coronal sections with vGluT2 and calculated the volume of the vGluT2-positive ChR2-expressing CN axon terminals (Fig. 4E; see Suppl. Material and Methods). This morphological reconstruction indicated that the size of the CN terminals in *tottering* mice ranges widely throughout VL, VM, CL/CM and ZI (Fig. 4F). We found that the smallest terminals, which often appeared '*en passant*' type, are located in ZI (0.96 ± 0.05 μm^3; 199 terminals from 4 mice) compared to VL (2.42 ± 0.95 μm^3; 903 terminals from 4 mice), VM (2.09 ± 0.63 μm^3; 691 terminals from 4 mice) and CL/CM (1.83 ± 0.73 μm^3; 230 terminals for 4 mice) ($p = 0.08$, MANOVA; see Suppl. Table 7). Collectively, these data indicate that direct optogenetic stimulation of CN is a more efficient in stopping seizures than stimulating a portion of CN axons and their variably sized axon terminals within the thalamic nuclei.

Stimulation of CN neurons induces heterogeneous effects in thalamus during interictal periods

To investigate the heterogeneity of the effects of CN stimulation on thalamic activity, we next set out to record single-unit thalamic neurons and evaluate the responses to CN stimulation during interictal periods (Fig. 5A; see Suppl. Fig. 2 for topographic mapping of cerebellar optic fibers). Out of 201 recorded neurons, 165 neurons were responsive to single-pulse CN stimulation with variable response latencies and types of responses (Fig. 5B–D; Suppl. Fig. 4; Suppl. Table 8). Upon CN stimulation 114 out of 165 neurons (69.1%) significantly increased their firing rate (group 'increased'; onset latency 21.3 ± 1.3 ms; duration response 47.0 ± 4.6 ms). Of these 114 cells, 24 showed a persisting effect (duration response: 94.7 ± 12.9 ms). Eighteen thalamic neurons (out of 165; 10.9%) responded in a bi-phasic manner, i.e., an initial increased firing rate followed by a significantly decreased firing rate (group 'bi-phasic'; onset latency increased phase: 15.5 ± 3.5 ms; duration response: 28.1 ± 3.7 ms; onset latency decreased phase: 60.2 ± 6.1 ms; average length of decrease of 196 ± 56 ms). A third cluster of 15 thalamic neurons (9.1%) only showed a decrease in firing rate upon CN stimulation (group 'decreased'; onset latency 20.6 ± 4.8 ms; length: 171 ± 51 ms). Finally, 18 recorded neurons (10.9%) did not show any significant change in firing rate during the 50-ms stimulus, but only thereafter (group 'delayed'; onset latency 68.4 ± 2.9 ms; length: 85.5 ± 9.3 ms). Interestingly, the number of spikes that was induced during an optogenetic pulse correlated negatively with the pre-stimulus firing frequency (Fig. 5C). Post hoc immunohistochemical analysis of the recording locations revealed that the individual nuclei in the thalamus all showed at least two

different types of responses (Fig. 5E; Suppl. Information). These findings indicate that CN stimulation evokes remarkably variable thalamic responses that are not restricted to a particular thalamic nucleus.

To find out how desynchronizing thalamic firing upon CN stimulation may translate into changes in cerebral cortical activity, we further analyzed the simultaneously recorded M1 and S1 ECoG activity (Fig. 6A). CN stimulation during interictal periods induced a large amplitude ECoG peak with high power in lower frequency bands (Suppl. Fig. 5). To optimize ECoG analysis during the post-stimulus period, we replaced the CN-evoked ECoG peak with baseline ECoG data (see 'Interictal ECOG Analysis' in Suppl. Material and Methods section). Hereby, we avoided any dominant effect of the CN-evoked low-frequency peak on the ECoG spectrogram, which lasts for a prolonged period of time (Suppl. Fig. 3) [15,35]. This replacement revealed that single-pulse CN stimulation during interictal periods resulted in a prolonged decrease in nearly all frequency bands (Fig. 6B–D; Suppl. Table 9). These data also showed that within the θ*-band (7–10 Hz), which corresponds to the frequency band most dominantly increased during absence seizures [36], power significantly reduced in ~40% of the trials - an effect seen at all recorded cortices (rM1: 39.9 ± 6.8%; lM1: 40.4 ± 6.3%; lS1: 40.4 ± 7.0%) in average responses and power spectrograms (Fig. 6C and D). Together, our data during interictal periods highlight the possibility that variability of thalamic responses to CN stimulation facilitates the desynchronizing effect of the CN on thalamic activity during seizures and that this impact can transverse towards the cerebral cortex.

Discussion

Using a combination of electrophysiology, pharmacology and optogenetics, we showed that CN stimulation elicits heterogeneous effects throughout the complex of thalamic nuclei in *tottering* mice, a well-established genetic model for generalized absence epilepsy [19,37]. Activation of the cerebello-thalamic pathway during seizures in *tottering* mice resulted in desynchronization of ictal thalamic activity. Moreover, increasing the regularity and firing frequency of CN neurons by pharmacological blockage of inhibitory input in the cerebellum (c.f., Fig. 2C in Ref. [15]) decimated thalamic burst firing without changing the average thalamic firing frequency and stopped the occurrence of GSWDs. Comparing the inter-ictal ECoG before and after cerebellar gabazine infusion revealed that indeed the power at the frequency range of 7–10 Hz was decreased. Given that short-lasting CN stimulation during interictal periods had a variety of effects on thalamic spiking, but still reduced the ECoG power at 7–10 Hz, these results indicate that cerebellar output is of relevance for controlling thalamo-cortical synchronicity in the frequency band of absence seizures.

Our multi- and single-unit recordings in *tottering* mice demonstrated that thalamic action potential firing is prominently phase-locked to GSWDs, which is in line with earlier reports on cellular excitability and hypersynchronicity in thalamo-cortical networks [38–41]. Single-unit recordings in primary, associative and intralaminar thalamic nuclei showed that ~50% of the neurons fire most action potentials ~20 ms prior to the peak of the ECoG spikes during GSWD episodes. In other rodent models of absence epilepsy the distribution of this delay also is rather narrow, ranging from 9 ms in a genetic rat model for absence epilepsy (GAERS) to 28 ms in Long-Evans rats [42,43]. Notably, we found that 54 of the 122 recorded thalamic neurons did not show significant modulation of their spiking pattern during GSWD episodes, which might be due to a decreased action potential firing in thalamus during GSWDs, as was previously highlighted in the GAERS model [44,45].

We found that long-lasting pharmacological blockage of local GABA-mediated transmission was effective in dampening the occurrence of GSWDs, but without affecting the average firing frequency of thalamic neurons. This absence of an effect on the thalamic spiking frequency appears counterintuitive in view of the increased firing frequency of CN neurons following local gabazine injections [15]. Although future experiments should investigate the underlying mechanism, two factors may contribute to the steady firing frequency of thalamic neurons during cerebellar pharmacological manipulations: (1) thalamic neurons receive inhibitory input from intrathalamic reticular and extrathalamic mesencephalic nuclei [46], which in principle could balance the impact of an

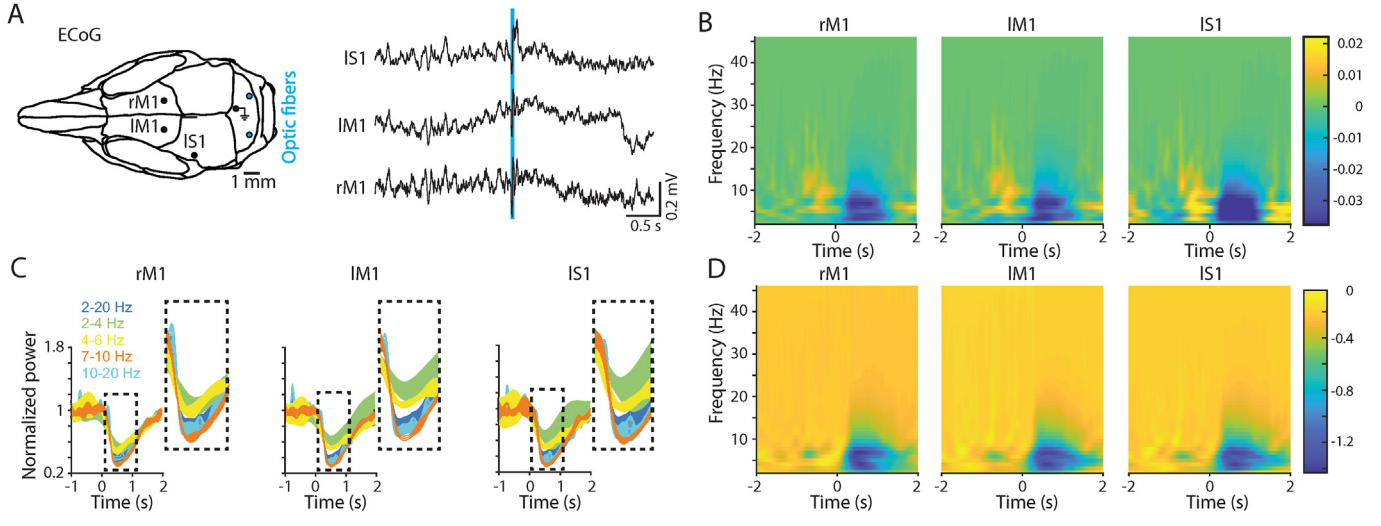

Fig. 6. CN stimulation dampens the power in ECoG frequency bands during interictal periods. (A) (*Left*) Placement of craniotomies for ECoG recording electrodes and optic fibers in the CN. (*Right*) Example ECoG trace from left S1 (lS1), left M1 (lM1) and right M1 (rM1) suggesting widespread effect of bilateral single-pulse optogenetic CN stimulation (50 ms at 0.2 Hz). (B) Normalized ECoG spectrogram from a single mouse (n = 246 stimuli) calculated after the masking of the large-amplitude ECoG response directly following CN stimulation to accurately analyze post-stimulus responses in all frequency bands (see also Suppl. Fig. 5). The color scale represents the ECoG power. This procedure is also applied to panels C and D. Note the clear drop in all frequency bands. (C) Normalized power in the individual frequency bands for all data (N = 7 mice), indicating that in all recorded cortices, single-pulse CN stimulation resulted in a significant ECoG spectral power decrease in all channels in rM1 θ (4–7 Hz), θ* (7–10 Hz), β (10–20 Hz), and the broadband 2–20 Hz, but not in rM1 δ- (2–4 Hz) and γ (25–40 Hz) bands (see Suppl. Table 9 for statistics). (D) Normalized spectrogram of the data represented in panel C (data from N = 7 mice). (For interpretation of the references to color in this figure legend, the reader is referred to the Web version of this article.)

increased CN firing frequency on the thalamic firing pattern; and (2) CN-thalamic synapses are excitatory, but have been shown in wild type rodents to be subject to paired-pulse depression when stimulated repetitively (e.g. Refs. [16,47]). It might be that the P601L loss-of-function mutation in $Ca_V2.1$ (P/Q-type) Ca^{2+} channels [37] weakens the synaptic transmission at CN-thalamic synapses and thereby contributes to the lack of impact of cerebellar gabazine infusions on thalamic firing frequency.

In our multi-unit recordings in freely behaving *tottering* mice we noticed that the peaks in thalamic firing during GSWDs, which highlight synchronous action potential firing, were dampened following optogenetic CN stimulation. This desynchronizing effect may be due to the heterogeneity of type, length and amplitude of the thalamic responses. In our head-fixed setup for single-unit recordings we recorded four different types of responses in thalamic firing patterns of which the most commonly recorded one was an increased firing pattern. In addition, a more complex and longer lasting change in firing pattern was recorded in 30% of the recorded neurons. On average the length of these 'decreased', 'biphasic' and 'delayed' responses outlasted the 50-ms optical stimulation by > 100 ms. This indicates that for ~150 ms the firing pattern of a substantial portion of thalamic neurons is desynchronized. Since in *tottering* mice cerebello-thalamo-cortical oscillations occur at ~8 Hz, i.e., with a cycle period of 125-ms, our data indicate that the synchronous oscillations of action potential firing and presumably also the membrane potential, are disrupted in 30% of the thalamic cells that receive CN input. Moreover, since thalamic depolarization has been proven effective in stopping thalamo-cortical oscillations characteristic of absence seizures in Wistar Albino Glaxo rats from Rijswijk (*WAGRij*) [48], also the relatively short-lasting 'increased' responses in principle could have a long-lasting effect by stopping the 125-ms cycle period of thalamic membrane potential oscillations. Finally, we also noted that the differences in amplitude of the responses, i.e., the absolute change in the firing rates, among individual neurons of the different response types are substantial. Given that we found at least two types of responses in neuronal firing in all thalamic nuclei, our data indicate that despite the pure excitatory nature of cerebello-thalamic synapses, neighboring thalamic cells respond variably to CN stimulation [16,35,47,49–56].

One possible source for the variability in the length and amplitude of the responses might be the fact that we infected neurons with ChR2 in various CN subregions (including medial, interposed and lateral nuclei) and that it was unavoidable to have some variability in the placement of the optical fibers (see Fig. 5 and Suppl. Fig. 2), thereby activating various neural networks that differentially evoke activity in the thalamus. This possibility is supported by the broad range of strengths that is reported for cerebello-thalamic synapses in wild type VL, VM and CL thalamus [16]. Additionally, the variability in the responses may in part result from the heterogeneous and variable impacts of the various indirect pathways between CN neurons and the recorded thalamic neurons. Indeed, the indirect projections from the CN to prethalamic nuclei, such as the middle and deeper layers of the superior colliculus, the zona incerta as well as the anterior pretectal nucleus, may contribute to the variability of thalamic responses to CN stimulation [17,46]. Moreover, these indirect pathways may, in conjunction with the intra-thalamic inhibitory projections from the reticular thalamic nucleus, explain why electrical CN stimulation can result in bi-modal excitatory-inhibitory responses in thalamus neurons [55,57,58]. Finally, it is also possible that excitation of CN neurons that do not project to thalamus, but rather to premotor nuclei in the brainstem, affect thalamo-cortical synchrony by eliciting proprioceptive signals that are indirectly evoked by motor responses [59–61].

Selective stimulation of a subpopulation of CN axons within the various thalamic nuclei turned out to be less efficient in stopping absence seizures than direct stimulation in the cerebellar nuclei. This may partially result from incomplete optogenetic control of the widespread CN terminals in the thalamic nuclei, compared to the direct targeting of localized neurons within the CN. In addition, it may be that the variability in CN axon terminal volume, which has been shown to be quite pronounced between VL, VM and CL/CM and to be linked to the amplitude of post-synaptic responses in wild type mice [16], also contributes to the lower number of seizures that were stopped by optical stimulation of ChR2-expressing CN axons in thalamic nuclei. Since direct stimulation in CN was most efficient, this might indicate that simultaneously evoking different activity patterns in multiple CN-thalamic pathways operates as a synergistic tool that via a divergent projection pattern effectively desynchronizes GSWDs.

In conclusion, our data show that targeted stimulation of CN neurons results in desynchronization of thalamic firing concurring with termination of GSWDs in *tottering* mice. This identifies the CN as a potentially important node in the neuronal network underlying generalized absence seizures, with potentially promising implications for other types of generalized seizures.

Funding

This research was supported by funding from ERC-Adv, ERC-PoC to C.I.D.Z., NWO-Veni and Erasmus MC fellowship to L.K., various ZonMw and NWO-ALW grants to A.M.J.M.v.d.M., C.I.D.Z. and F.E.H, FP7 "EUROHEADPAIN" to A.M.J.M.v.d.M. and EU IAPP "BRAINPATH" to A.M.J.M.v.d.M. and E.A.T., EU Marie Curie Career Integration Grant to E.A.T. and the Dutch National Epilepsy Foundation to A.M.J.M.v.d.M. and E.A.T. L.K., E.A.T., A.M.J.M.V.D.M, C.I.D.Z. and F.E.H. are supported by the national medical delta ('Medical Neurodelta)' scientific program, and finally C.I.D.Z. and L.K. are supported by the Crossover LSH-NWO grant INTENSE. F.E.H. is supported by the C.J. Vaillant Fund.

Potential competing interests

Nothing to report.

Credit author statement – Eelkman Rooda et al

O.H.J.E.R. performed all experiments with help of L.K, H.J.P. and N.A.J. for recordings and stimulations in head-fixed animals, of S.J.F. and E.A.T. for recordings in freely moving animals, of L.K. for seizure detection and analyses of spike modulation, of P.H. for analysis of ECoG activity, and of S.V.G. for axonal projection analyses; E.A.T., A.M.J.M.v.d.M. and C.I.D.Z. contributed to experimental setups, supervised the project and provided financial support; O.H.J.E.R., L.K. and F.E.H. conceived and designed experiments; O.H.J.E.R., L.K., C.I.D.Z. and F.E.H. wrote the manuscript with help from all co-authors.

Declaration of competing interest

None.

Acknowledgements

The authors thank Elize Haasdijk, Erika Sabel-Goedknegt, Mandy Rutteman, Marloes Adank, Jinne Geelen, Beerend Winkelman, Maarten Schenke and Farnaz Nassirinia for excellent technical and analytical support and Thijs Houben, Bas van Hoogstraten,

Daniël Dumas, Carmen Schäfer, Sander Lindeman, Zhenyu Gao, and Saša Peter for their practical and insightful comments.

Appendix A. Supplementary data

Supplementary data to this article can be found online at https://doi.org/10.1016/j.brs.2021.05.002.

References

[1] Fogerson PM, Huguenard JR. Tapping the brakes: cellular and Synaptic Mechanisms that regulate thalamic oscillations. Neuron 2016;92(4):687–704.
[2] Aarabi A, Wallois F, Grebe R. Does spatiotemporal synchronization of EEG change prior to absence seizures? Brain Res 2008;1188:207–21.
[3] Adebimpe A, Aarabi A, Bourel-Ponchel E, Mahmoudzadeh M, Wallois F. Functional brain dysfunction in patients with benign childhood epilepsy as revealed by graph theory. PloS One 2015;10(10).
[4] Beenhakker MP, Huguenard JR. Neurons that fire together also conspire together: is normal sleep circuitry hijacked to generate epilepsy? Neuron 2009;62(5):612–32.
[5] Cressman JR, Ullah G, Ziburkus J, Schiff SJ, Barreto E. The influence of sodium and potassium dynamics on excitability, seizures, and the stability of persistent states: I. Single neuron dynamics. J Comput Neurosci 2009;26(2):159–70.
[6] Danober L, Deransart C, Depaulis A, Vergnes M, Marescaux C. Pathophsyiological mechanisms of genetic absence epilepsy in the rat. Prog Neurobiol 1998;55(1):27–57.
[7] Kobau R, Zahran H, Thurman DJ, Zack MM, Henry TR, Schachter SC, et al. Epilepsy surveillance among adults–19 states, behavioral risk factor surveillance system. Morbidity and mortality weekly report Surveillance summaries 2008 2005;57(6):1–20.
[8] Kwan P, Schachter SC, Brodie MJ. Drug-resistant epilepsy. N Engl J Med 2011;365(10):919–26.
[9] Fisher RS, Velasco AL. Electrical brain stimulation for epilepsy. Nat Rev Neurol 2014;10(5):261–70.
[10] Sprengers M, Vonck K, Carrette E, Marson AG, Boon PAJM. Deep brain and cortical stimulation for epilepsy. Cochrane Database Syst Rev 2017;7.
[11] Fisher RS, Salanova V, Witt T, Worth R, Henry T, Gross R, et al. Electrical stimulation of the anterior nucleus of thalamus for treatment of refractory epilepsy. Epilepsia 2010;51(5):899–908.
[12] Salanova V, Witt T, Worth R, Henry T, Gross R, Nazzaro J, et al. Long-term efficacy and safety of thalamic stimulation for drug-resistant partial epilepsy. Neurology 2015;84(10):1017–25.
[13] Fisher RS, Acevedo C, Arzimanoglou A, Bogacz A, Cross JH, Elger CE, et al. ILAE official report: a practical clinical definition of epilepsy. Epilepsia 2014;55(4):475–82.
[14] Kros L, Eelkman Rooda OHJ, De Zeeuw CI, Hoebeek FE. Controlling cerebellar output to treat refractory epilepsy. Trends Neurosci 2015;38(12):787–99.
[15] Kros L, Eelkman Rooda OHJ, Spanke JK, Alva P, Van Dongen MN, Karapatis A, et al. Cerebellar output controls generalized spike-and-wave discharge occurrence. Ann Neurol 2015;77(6):1027–49.
[16] Gornati SV, Schafer CB, Eelkman Rooda OHJ, Nigg AL, De Zeeuw CI, Hoebeek FE. Differentiating cerebellar impact on thalamic nuclei. Cell Rep 2018;23(9):2690–704.
[17] Schafer CB, Hoebeek FE. Convergence of primary sensory cortex and cerebellar nuclei pathways in the whisker system. Neuroscience 2018;368:229–39.
[18] Teune TM, Van der Burg J, Van der Moer J, Ruigrok TJ. Topography of cerebellar nuclear projections to the brain stem in the rat. Prog Brain Res 2000;124:141–72.
[19] Noebels JL, Sidman RL. Spike-Wave and focal motor seizures in the mutant mouse tottering. Science 1979;204(4399):1334–6.
[20] Mattis J, Tye KM, Ferenczi EA, Ramakrishnan C, O'Shea DJ, Prakash R, et al. Principles for applying optogenetic tools derived from direct comparative analysis of microbial opsins. Nat Methods 2012;9(2):159–72.
[21] Gradinaru V, Mogri M, Thompson KR, Henderson JM, Deisseroth K. Optical deconstruction of parkinsonian neural circuitry. Science 2009;324(5925):354–9.
[22] Houben T, Loonen IC, Baca SM, Schenke M, Meijer JH, Ferrari MD, et al. Optogenetic induction of cortical spreading depression in anesthetized and freely behaving mice. J Cerebr Blood Flow Metabol 2017;37(5):1641–55.
[23] University S. Predicted irradiance values: model based on direct measurements in mammalian brain tissue. http://web.stanford.edu/group/dlab/cgi-bin/graph/chart.php. [Accessed 16 April 2016].
[24] Van Dongen MN, Hoebeek FE, Koekkoek SKE, De Zeeuw CI, Serdijn W. High frequency switched-mode stimulation can evoke post synaptic responses in cerebellar principal neurons. Front Neuroeng 2015;8(2) [Epub].
[25] Holt GR, Softky WR, Koch C, Douglas RJ. Comparison of discharge variability in vitro and in vivo in cat visual cortex neurons. J Neurophysiol (Bethesda) 1996;75(5):1806–14.
[26] Kundishora AJ, Gummadavelli A, Ma C, Liu M, McCafferty C, Schiff ND, et al. Restoring conscious arousal during focal limbic seizures with deep brain stimulation. Cerebr Cortex 2016;27(3):1964–75.
[27] Kandel A, Buzsáki G. Cerebellar neuronal activity correlates with spike and wave EEG patterns in the rat. Epilepsy Res 1993;16(1):1–9.
[28] Kros L, Lindeman SL, Eelkman Rooda OHJ, De Zeeuw CI, Hoebeek FE. Synchronicity and rhythmicity of Purkinje cell firing during generalized spike-and-wave discharges in a natural mouse model of absence epilepsy. Front Cell Neurosci 2017;11(346).
[29] Bentivoglio M, Kuypers HG. Divergent axon collaterals from rat cerebellar nuclei to diencephalon, mesencephalon, medulla oblongata and cervical cord. A fluorescent double retrograde labeling study. Exp Brain Res 1982;46(3):339–56.
[30] Kuramoto E, Ohno S, Furuta T, Unzai T, Tanaka YR, Hioki H, et al. Ventral medial nucleus neurons send thalamocortical afferents more widely and more preferentially to layer 1 than neurons of the ventral anterior-ventral lateral nuclear complex in the rat. Cerebr Cortex 2015;25(1):221–35.
[31] Kuramoto E, Furuta T, Nakamura KC, Unzai T, Hioki H, Kaneko T. Two types of thalamocortical projections from the motor thalamic nuclei of the rat: a single neuron-tracing study using viral vectors. Cerebr Cortex 2009;19(9):2065–77.
[32] Van Dongen MN, Karapatis A, Kros L, Eelkman Rooda OHJ, Seepers RM, Strydis C, et al. An implementation of a wavelet-based seizure detection filter suitable for realtime closed-loop epileptic seizure suppression. Lausanne: BioCAS; 2014. p. 504–7.
[33] Chen J, Kriegstein AR. A GABAergic projection from the zona incerta to cortex promotes cortical neuron development. Science 2015;350(6260):554–8.
[34] Valentin A, Garcia Navarrete E, Chelvarajah R, Torres C, Navas M, Vico L, et al. Deep brain stimulation of the centromedian thalamic nucleus for the treatment of generalized and frontal epilepsies. Epilepsia 2013;54(10):1823–33.
[35] Proville RD, Spolidoro M, Guyon N, Dugué GP, Selimi F, Isope P, et al. Cerebellum involvement in cortical sensorimotor circuits for the control of voluntary movements. Nat Neurosci 2014;17(9):1233–9.
[36] Sorokin JM, Paz JT, Huguenard JR. Absence seizure susceptibility correlates with pre-ictal B oscillations. J Physiol Paris 2016;110:372–81.
[37] Fletcher CF, Lutz CM, O'Sullivan TN, Shaughnessy JD, Hawkes R, Frankel WN, et al. Absence epilepsy in tottering mutant mice is associated with calcium channel defects. Cell 1996;87(4):607–17.
[38] Zhang Y, Mori M, B DL, Noebels JL. Mutations in high-voltage activated calcium channel genes stimulate low-voltage-activated currents in mouse thalamic relay neurons. J Neurosci 2002;22(15):6362–71.
[39] Song I, Kim D, Choi S, Sun M, Kim Y, Shin HS. Role of the A1G T-type calcium channel in spontaneous absence seizures in mutant mice. J Neurosci 2004;24(22):5249–57.
[40] Sasaki S, Huda K, Inoue T, Miyata M, Imoto K. Impaired feedforward inhibition of the thalamocortical projection in epileptic Ca2+ channel mutant mice, tottering. J Neurosci 2006;26(11):3056–65.
[41] Depaulis A, Charpier S. Pathophysiology of absence epilepsy: insights from genetic models. Neurosci Lett 2017.
[42] Polack PO, Charpier S. Intracellular activity of cortical and thalamic neurones during high-voltage rhythmic spike discharge in Long-Evans rats in vivo. J Physiol 2006;571:461–76.
[43] Polack PO, Mahon S, Chavez M, Charpier S. Inactivation of the somatosensory cortex prevents paroxysmal oscillations in cortical and related thalamic neurons in a genetic model of absence epilepsy. Cerebr Cortex 2009;19(9):2078–91.
[44] McCafferty C, David F, Venzi M, Lorincz ML, Delicata F, Atherton Z, et al. Cortical drive and thalamic feed-forward inhibition control thalamic output synchrony during absence seizures. Nat Neurosci 2018;21(5):744–56.
[45] Slaght SJ, Leresche N, Deniau JM, Crunelli V, Charpier S. Activity of thalamic reticular neurons during spontaneous genetically determined spike and wave discharges. J Neurosci 2002;22(6):2323–34.
[46] Halassa MM, Acsady L. Thalamic inhibition: diverse sources, diverse scales. Trends Neurosci 2016;39(10):680–93.
[47] Sawyer SF, Young SJ, Groves PM, Tepper JM. Cerebellar-responsive neurons in the thalamic ventroanterior-ventrolateral coplex of rats: in vivo electrophysiology. Neuroscience 1994;63:711–24.
[48] Sorokin JM, Davidson TJ, Frechette E, Abramian AM, Deisseroth K, Huguenard JR, et al. Bidirectional control of generalized epilepsy networks via rapid real-time switching of firing mode. Neuron 2017;93(1):194–210.
[49] Aumann TD, Horne MK. Ramification and termination of single axons in the cerebellothalamic pathway of the rat. J Comp Neurol 1996;376:420–30.
[50] Chevalier G, Deniau JM. Inhibitory nigral influence on cerebellar evoked responses in the rat ventromedial thalamic nucleus. Exp Brain Res 1982;48(3):369–76.
[51] Cohen D, Chambers WW, Sprague JM. Experimental study of the efferent projections from the cerebellar nuclei to the brainstem of the cat. J Comp Neurol 1958;109(2):233–59.
[52] Popa D, Spolidoro M, Proville RD, Guyon N, Belliveau L, Léna C. Functional role of the cerebellum in gamma-band synchronization of the sensory and motor cortices. J Neurosci 2013;33(15):6552–6.
[53] Sasaki K, Matsuda Y, Mizuno N. Distribution of cerebellar-induced responses in the cerebral cortex. Exp Neurol 1973;39(2):342–54.
[54] Steriade M, Contreras D. Relations between cortical and thalamic cellular events during transition from sleep patterns to paroxysmal activity. J Neurosci 1995;15(1):623–42.
[55] Uno M, Yoshida M, Hirota I. The mode of cerebello-thalamic relay transmission investigated with intracellular recording from cells of the ventrolateral nucleus of cat's thalamus. Exp Brain Res 1970;10(2):121–39.

[56] Yoshida M, Yajima K, Uno M. Different activation of the 2 types of the pyramidal tract neurones through the cerebello-thalamocortical pathway. Experientia 1966;22(5):331–2.
[57] Bava A, Cicirata F, Giuffrida R, Licciardello S, Panto MR. Electrophysiologic properties and nature of ventrolateral thalamic nucleus neurons reactive to converging inputs of paleo- and neocerebellar origin. Exp Neurol 1986;91(1):1–12.
[58] Bava A, Manzoni T, Urbano A. Effects of fastiginal stimulation on thalamic neurones belonging to the diffuse projection system. Brain Res 1967;4(4):378–80.
[59] Witter L, Canto CB, Hoogland TM, de Gruijl JR, De Zeeuw CI. Strength and timing of motor responses mediated by rebound firing in the cerebellar nuclei after Purkinje cell activation. Front Neural Circ 2013;7:133.
[60] Hoogland TM, De Gruijl JR, Witter L, Canto CB, De Zeeuw CI. Role of synchronous activation of cerebellar purkinje cell ensembles in multi-joint movement control. Curr Biol 2015;25(9):1157–65.
[61] Yu C, Derdikman D, Haidarliu S, Ahissar E. Parallel thalamic pathways for whisking and touch signals in the rat. PLoS Biol 2006;4(5):e124.